CrystEngComm

Cite this: *CrystEngComm*, 2012, **14**, 684

www.rsc.org/crystengcomm

PAPER

Selective carbon dioxide uptake and crystal-to-crystal transformation: porous 3D framework to 1D chain triggered by conformational change of the spacer†

Ritesh Haldar[a] **and Tapas Kumar Maji***[ab]

Received 7th July 2011, Accepted 27th September 2011
DOI: 10.1039/c1ce05847a

α-Po type 3D porous frameworks, $\{[M(bpe)_2(N(CN)_2)]N(CN)_2 \cdot xH_2O\}_n$, (M = Zn(II) ($x = 5$) (**1**)/Co(II) ($x = 4$) (**2**)) (bpe = 1,2-bis(4-pyridyl)ethane, $N(CN)_2^-$ = dicyanamide anion) composed of mixed ligand systems have been synthesized and structurally characterized. Upon two-fold interpenetration both 3D frameworks **1** and **2** show a bimodal channel structure; the small channels contain non-coordinated $N(CN)_2^-$ anions and the bigger channels are occupied by guest water molecules. High framework stability for both compounds was realized by similarity in the PXRD pattern in dehydrated state and even a reversible single-crystal-to-single-crystal transformation for framework **1**. Both the frameworks display unprecedented structural transformation from 3D framework to 1D $\{[M(bpe)(N(CN)_2)_2]\}_n$ (M = Zn(II) (**1b**)/Co(II) (**2b**)) coordination chain upon removal of one molecule of bpe and concomitant bridging of non-coordinated $N(CN)_2^-$ and conformational change (*anti* to *gauche*) by another bridging bpe linker. Moreover, the dehydrated solid $\{[Co(bpe)_2(N(CN)_2)]N(CN)_2\}_n$ (**2a**) exhibits highly selective CO_2 uptake relative to a number of adsorbates (H_2, N_2, O_2 and Ar) at 195 K.

Introduction

Metal–organic frameworks (MOFs) or porous coordination polymers (PCPs) are a new class of solid-state material featuring regular and designable channel structure with permanent porosity composed of flexible coordination bonds.[1] The last couple of decades have witnessed enormous growth in the field of MOFs and many interesting properties and applications have been unveiled including gas storage and separation,[2] heterogeneous catalysis,[3] ion exchange[4] and drug delivery.[5] Apart from these critical applications, single-crystal-to-single-crystal transformation[6] and solid-state structural conversion is one of the key observation in flexible MOFs induced by external stimuli, *e.g.*, light, heat, pressure, guest *etc*.[7] Much effort has been devoted for preparing environmentally responsive materials, and a variety of crystal-to-crystal transformations, such as 0D → 1D/2D, 1D → 2D, 2D → 3D have been documented.[8] These type of structural transformations are associated with the cleavage and generation of new coordination bonds and the corresponding change in dimensionality is reflected by subtle changes in porosity, optical and magnetic properties.[9] Crystal-to-crystal transformations 3D → 2D, 3D → 1D or 2D → 1D are yet to be realized in metal–organic framework materials.

The recognition and selective adsorption of gas molecules by MOFs are of paramount importance in particular environmental and industrial fields. The rapid growth of the atmospheric carbon dioxide (CO_2) level, mainly from the emission of fossil fuel based power plants demands an urgent strategy that can selectively sequester and store the greenhouse gas CO_2. The current conventional techniques for flue gas sequestrations, such as amine absorbers and cryogenic coolers are not a permanent solution in the long run due to low efficacy and economic drawbacks.[10] In this context MOFs are being studied to address these challenges because it is possible to design a framework which can selectively recognize specific molecules by various host–guest interactions resulting in selective adsorption characteristics.[11] Already, a few examples of MOFs with selective CO_2 uptake have been reported by tuning the pore size and introducing the specific functionality in the organic spacer, which interact effectively with the CO_2 molecule.[12]

Here, in this article, we report the synthesis, structural characterization and crystal-to-crystal transformation of two isostructural two-fold interpenetrated α-polonium type 3D porous coordination frameworks, $\{[M(bpe)_2(N(CN)_2)]N(CN)_2 \cdot xH_2O\}_n$ (M = Zn(II) ($x = 5$) (**1**)/Co(II) ($x = 4$) (**2**)) (bpe = 1,2-bis(4-pyridyl)ethane, $N(CN)_2^-$ = dicyanamide), which are isostructural to earlier reported $\{[Ni(bpe)_2(N(CN)_2)]N(CN)_2 \cdot 6H_2O\}_n$ compound.[13] Both the frameworks exhibit unprecedented 3D → 1D structural transformation by release of one bpe and concomitant conformational change from *anti* to *gauche* by

[a]*Molecular Materials Laboratory, New Chemistry Unit, Jawaharlal Nehru Center for Advanced Scientific research, Jakkur, Bangalore, 560064, India. E-mail: tmaji@jncasr.ac.in; Fax: +91-80 22082766*
[b]*Chemistry and Physics of Materials Unit, Jawaharlal Nehru Center for Advanced Scientific research, Jakkur, Bangalore, 560064, India*

† Electronic supplementary information (ESI) available: Selected bond distances for all compounds, Experimental part, PXRD patterns, IR spectra, crystal structure figures and Indexing results. Crystallographic files for compounds **1**, **1′**, **1″** and **2** in CIF format. CCDC reference numbers 834078–834081. For ESI and crystallographic data in CIF or other electronic format see DOI: 10.1039/c1ce05847a

another bpe linker and coordination by free $N(CN)_2^-$ anion triggered by temperature. Dehydrated compound **2** (**2a**) shows excellent selective CO_2 gas uptake relative to other gases (N_2, H_2, O_2 and Ar) at 195 K.

Experimental

Materials

All the reagents employed were commercially available and used as provided without further purification. All the metal salts were obtained from Spectrochem, 1,2-bis(4-pyridyl)ethane and sodium dicyanamide were obtained from Sigma Aldrich chemicals.

Physical measurements

Elemental analysis was carried out using a Thermo Fischer Flash 2000 Elemental Analyzer. IR spectra were recorded on a Bruker IFS 66v/S spectrophotometer using KBr pellets in the region 4000–400 cm^{-1}. Thermogravimetric analysis (TGA) was carried out (Metler Toledo) in nitrogen atmosphere (flow rate = 50 ml min^{-1}) in the temperature range 30–500 °C (heating rate = 3 °C min^{-1}). Powder XRD pattern of the products were recorded by using Mo-Kα radiation (Bruker D8 Discover; 40 kV, 30 mA). The pattern was agreed with those calculated from single crystal structure determination.

Synthesis of $\{[M(bpe)_2(N(CN)_2)]N(CN)_2 \cdot xH_2O\}_n$ (M = Zn(II) ($x = 5$) (1)/Co(II) ($x = 4$) (2))

An aqueous solution (25 mL) of $NaN(CN)_2$ (1 mmol, 0.089 g) was mixed with an ethanolic solution (25 mL) of bpe (1 mmol, 0.184 g) and stirred well for 30 min. $Zn(NO_3)_2 \cdot 6H_2O$ (0.5 mmol, 0.146 g) (for compound **2**, $Co(NO_3)_2 \cdot 6H_2O$) was dissolved in 50 mL of water and added to the ligand solution dropwise. White (**1**) and orange (**2**) powder samples were isolated after 1–2 days of continuous stirring. Just by keeping the filtrate solution in room temperature for 4–5 days beautiful colorless (for **1**) and orange colored (for **2**) block shaped crystals were obtained. The crystals were separated, washed with water and dried. Good quality single crystals were picked up from the mother-liquor and immediately covered with paraffin oil and crystal data was collected at 293 K. Compound **1**: Yield: 68%, relative to Zn. FT-IR (KBr pellet, 4000–400 cm^{-1}): 3492(br), 3234(w), 3070(w), 2330(s), 2232(m), 2126(m), 1610(s), 1568(s), 1502(s), 1424(s), 1311(w), 1223(s), 1065(s), 1021(s), 910(w), 872(w), 829(s). Anal. Calc. for $C_{28}H_{34}ZnN_{10}O_5$: C, 51.26; H, 5.19; N, 21.35. Found: C, 52.11; H, 5.17; N, 21.01%. Compound **2**: Yield: 70%, relative to Co. FT-IR (KBr pellet, 4000–400 cm^{-1}): 3490(br), 3234(w), 3072 (w), 2326(s), 2238(m), 2128(m), 1614(s), 1562(s), 1502(s), 1428(s), 1310(w), 1228(s), 1068(s), 1020(s), 912(w), 874(w), 820(s). Anal. Calc. for $C_{28}H_{32}CoN_{10}O_4$: C, 53.24; H, 5.07; N, 22.18. Found: C, 52.91; H, 5.03; N, 21.79%.

Preparation of $\{[Zn(bpe)_2(N(CN)_2)]N(CN)_2 \cdot H_2O)\}_n$ (1′) and $[Zn(bpe)_2(N(CN)_2)]N(CN)_2 \cdot 5H_2O)\}_n$ (1″)

A few good quality single crystals of compound **1** were kept in a glass sample cell and heated at 70 °C under dynamic vacuum (10^{-1} Pa) for 12 h. A good quality single crystal was separated and immediately covered with paraffin oil and crystal data was collected. The same dehydrated crystal (**1′**) was again exposed to water vapour for 1–2 days to obtain **1″** and crystal data was collected at 293 K.

Synthesis of $\{M(bpe)(N(CN)_2)_2\}_n$ (M= Zn(II) (1b)/Co(II) (2b)) from $\{[M(bpe)_2(N(CN)_2)]N(CN)_2 \cdot xH_2O)\}_n$ (M = Zn(II) ($x = 5$) (1)/Co(II) ($x = 4$) (2))

As-synthesized compound **1** (or **2**) (about 150 mg) was heated in a glass tube at 200 °C under dynamic vacuum (10^{-1} Pa) for about 6 h. White to light brown (**1**) and orange to red (**2**) color change was observed. The heated compounds were characterized by elemental analyses, IR and powder X-ray diffraction study. Compound **1b**: FT-IR (KBr pellet, 4000–400 cm^{-1}): 3232(w), 3067(w), 2296(s), 2247(s), 2181(s), 1610(s), 1560(s), 1500(s), 1429 (s), 1347(s), 1215(s), 1071(s), 1021(s), 928(m), 810 (s). Anal. Calc. for $C_{16}H_{12}ZnN_8$: C, 50.39; H, 3.14; N, 29.39. Found: C, 50.82; H, 3.54; N, 29.75%. Compound **2b**: FT-IR (KBr pellet, 4000–400 cm^{-1}): 3237(w), 3057(w), 2298(s), 2240(s), 2180(s), 1616(s), 1561(s), 1503(s), 1423(s), 1349(s), 1216(s), 1074(s), 1024(s), 928 (m), 807(s). Anal. Calc. for $C_{16}H_{12}CoN_8$: C, 51.16; H, 3.31; N, 29.84. Found: C, 51.51; H, 3.39; N, 29.09%.

X-Ray crystallography

X-Ray single-crystal structural data of **1**, **1′**, **1″** and **2** were collected on a Bruker Smart-CCD diffractometer equipped with a normal focus, 2.4 kW sealed tube X-ray source with graphite monochromated Mo-Kα radiation ($\lambda = 0.71073$ Å) operating at 50 kV and 30 mA. The program SAINT[14] was used for integration of diffraction profiles and absorption correction was made with SADABS[15] program. All the structures were solved by SIR92[16] and refined by full-matrix least-squares method using SHELXL-97.[17] In compound **1** the nitrogen atom (N5) of guest $N(CN)_2^-$ is in positional disorder and has been resolved in terms of their occupancy. In compound **1′** and **1″** N4 and N5 and, for compound **2** N2 and N6 atoms of bridging and guest $N(CN)_2^-$ are in positional disorder, respectively, and has been resolved in terms of their occupancy. All the hydrogen atoms were geometrically fixed and placed in ideal positions. Potential solvent accessible area or void space was calculated using the PLATON multipurpose crystallographic software.[18] All crystallographic and structure refinement data of **1**, **1′**, **1″** and **2** are summarized in Table 1. Selected bond lengths and angles for **1**, **1′**, **1″** and **2** are given in Table S1–S4, respectively (ESI†). All calculations were carried out using SHELXL 97,[17] PLATON,[18] SHELXS 97[19] and WinGX system, Ver 1.70.01.[20]

Adsorption study

The adsorption isotherm of CO_2, H_2, N_2, Ar and O_2 (195 K) using the dehydrated sample of **2** were measured by using a QUANTACHROME QUADRASORB-*SI* analyzer. In the sample tube was placed sample **2** (~100–150 mg) which had been prepared at 348 K under a 1×10^{-1} Pa vacuum for about 6 h prior to measurement of the isotherms. Helium gas (99.999% purity) at a certain pressure was introduced in the gas chamber and allowed to diffuse into the sample chamber by opening the

Table 1 Crystal data and structure refinement parameters of compound **1**, **1′**, **1″** and **2**

	1	**1′**	**1″**	**2**
Empirical formula	$C_{28}H_{34}ZnN_{10}O_5$	$C_{28}H_{26}ZnN_{10}O$	$C_{28}H_{34}ZnN_{10}O_5$	$C_{28}H_{32}CoN_{10}O_4$
M_r	655.96	583.96	655.96	631.50631.50
Crystal system	Monoclinic	Monoclinic	Monoclinic	Monoclinic
Space group	*C*2/*c*	*C*2/*c*	*C*2/*c*	*C*2/*c*
a/Å	18.5219(3)	18.7806(5)	18.5462(9)	18.5114(7)
b/Å	20. 0552(3)	19.9045(5)	20.0824(10)	20.0115(8)
c/Å	8.7707(1)	8.7871(2)	8.7759(5)	8.7093(3)
β/°	100.993(1)	100.981(1)	101.244(3)	100.555(2)
V/Å^3	3198.19(8)	3224.64(14)	3205.9(3)	3171(2)
Z	4	4	4	4
T/K	293	150	283	293
λ(Mo-Kα)	0.71073	0.71073	0.71073	0.71073
D_c/g cm^{-3}	1.342	1.199	1.338	1.306
μ/mm^{-1}	0.820	0.797	0.818	0.589
θ_{max}/°	25.5	26.4	27.5	32.1
Total data	18296	19272	17049	23902
Unique reflections	2979	3285	3683	1950
R_{int}	0.040	0.039	0.090	0.051
Data [$I > 2\sigma(I)$]	2583	2644	2444	4115
R	0.0587	0.0815	0.0809	0.0669
R_w	0.1836	0.2764	0.2649	0.2256
GOF	1.11	1.15	1.07	1.07

valve. The amount of gas adsorbed was calculated readily from pressure difference ($P_{calc} - P_e$), where P_{calc} is the calculated pressure with no gas adsorption and P_e is the observed equilibrium pressure. All operations were computer-controlled and automatic.

The adsorption of different vapors such as MeOH at 293 K and H_2O, EtOH at 298 K were measured in the dehydrated sample of **2** in the vapor state by using a BELSORP-aqua-3 analyzer. The sample of **2** (~100–150 mg) was prepared as above prior to measurement of the isotherms. The different solvent molecules used to generate the vapor were degassed fully by repeated evacuation. Dead volume was measured with helium gas. The adsorbate was placed into the sample tube, then the change of the pressure was monitored and the degree of adsorption was determined by the decrease in pressure at the equilibrium state. All operations were computer controlled and automatic.

Results and discussion

Crystal structure descriptions of 1 and 2

Compounds **1** and **2** both crystallize in the monoclinic *C*2/*c* space group (Table 1) and structure determination by X-ray crystallography reveals a 3D α-Po type coordination framework of M(II) (M = Zn(II) (**1**)/Co(II) (**2**)) bridged by bpe and $N(CN)_2^-$ linkers and are found to be isostructural with the Ni(II) analogue.[13] Each slightly distorted octahedral M(II) center is ligated with four nitrogen atoms from four bpe and two nitrogen atoms of two $N(CN)_2^-$ linkers (Fig. 1 and Fig. S1, ESI†). For **1** the Zn–N bond lengths are in the range of 2.155(5)–2.212(5) Å (Table S1, ESI†). Similarly, for compound **2**, Co–N bond lengths are in the range 2.113(3)–2.189(2) Å (Table S2, ESI†). The four bpe linkers linked to the M(II) center forms a 2D sheet of $\{M(bpe)_2\}^{2+}$ along the crystallographic *ab* plane which is pillared by $N(CN)_2^-$ resulting in a α-polonium type 3D framework (Fig. 1a and b; Fig. S2a and S2b, ESI†). The 3D framework undergoes two-fold interpenetration ensuing two distinct channels; hexagonal channel having dimension of 5.5 × 4.5 Å^2 (6 × 4.5 Å^2 for compound **2**)[21] houses guest water molecules and the rectangular one with dimension of 2.0 × 0.5 Å^2 (2.5 × 0.5 Å^2, for compound **2**) shelters $N(CN)_2^-$ anions (Fig. 2c and d; Fig. S2c and S2d, ESI† and Fig. 3). The conformationally flexible bpe remains in *anti* conformation with a dihedral angle of 176.37° (178.14° for compound **2**) along the ethane C–C bond. The Zn(II)···Zn(II) separation along the $N(CN)_2^-$ and bpe are 8.773 Å and 13.669 Å, respectively (8.709 and 13.630 Å respectively, for compound **2**). The effective solvent accessible void space was calculated using the PLATON[21] and amounts to 20.9% (for **1**) and 21.1% void space (for **2**) relative to the total crystal volume.

Framework stability: TG and PXRD analysis

TG analysis of compound **1** carried out under nitrogen atmosphere shows a weight loss of 10% (calc. ~12 wt%) in the range 30–75 °C, corresponding to the five guest water molecules, and the dehydrated framework is stable up to ~145 °C (Fig. 4;

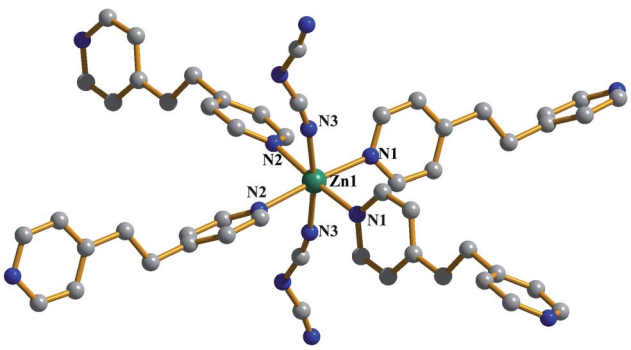

Fig. 1 View of the coordination environment of Zn(II) in compound **1**.

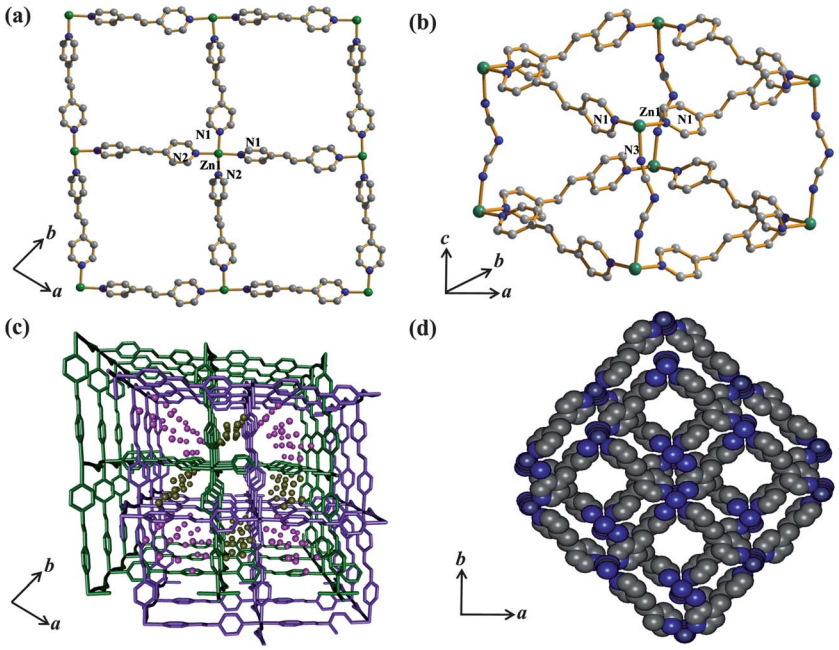

Fig. 2 (a) 2D sheet of $\{Zn(bpe)_2\}^{2+}$ along the crystallographic *ab* plane, (b) α-Po type 3D building unit of compound **1**, (c) View of 3D framework along the crystallographic *c*-axis showing two-fold interpenetrated bimodal channel structure, (d) CPK diagram showing two types of pores along *c* axis.

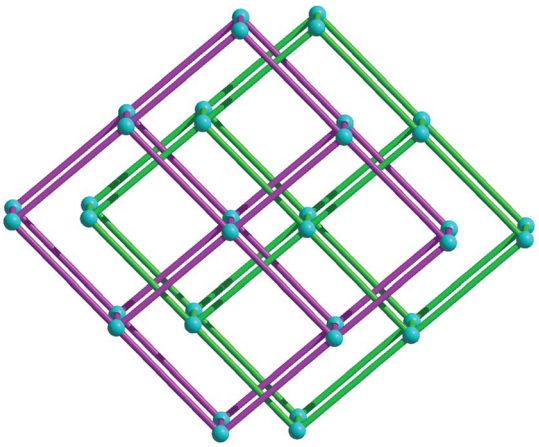

Fig. 3 α- Polonium type topology of compound $\{[M(bpe)_2(N(CN)_2)]N(CN)_2 \cdot xH_2O\}_n$ (M = Zn(II) (*x* = 5) (**1**)/Co(II) (*x* = 4) (**2**)).

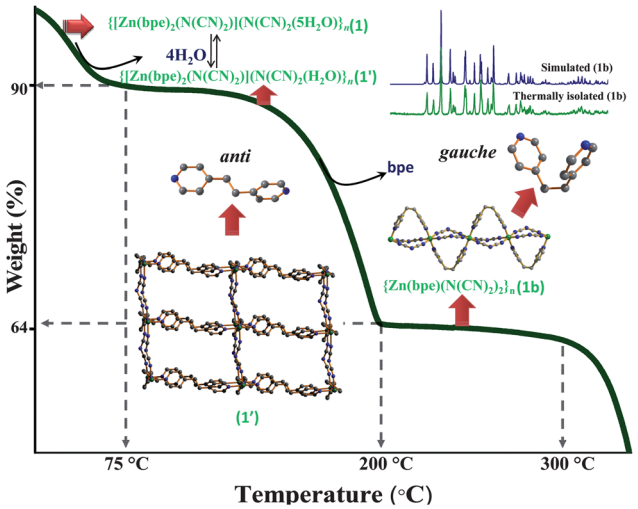

Fig. 4 Schematic representation of 3D ($\{[Zn(bpe)(N(CN)_2)_2]N(CN)_2 \cdot 5H_2O)\}_n$ (**1**) to 1D $\{[Zn(bpe)(N(CN)_2)_2]\}_n$ (**1b**) crystal-to-crystal transformation triggered by release of the one coordinated bpe linker. PXRD pattern of thermally isolated product and as-synthesized compound **1b**. 1D coordination chain of $\{Zn(bpe)(N(CN)_2)_2\}_n$ (**1b**).

Fig. S3, ESI†). The slight discrepancy in the weight loss can be correlated to the release of loosely bound water molecules at RT in the powder sample. Then, in the range of 150–200 °C a significant weight loss of 26% was observed which corresponds to the loss of one bpe linker and this particular phase is stable up to 280 °C without further weight loss. Upon further heating another bpe was released at ~340 °C, and then decomposition to unidentified product occurred. TG analysis of compound **2** (Fig. S4, ESI†) also shows a weight loss of 10% (calc. ~11 wt%) in the range 30–80 °C, corresponding to the four guest water molecules, and the dehydrated framework is stable up to ~140 °C. Then, in the range of 150–210 °C a significant weight loss of 26% was observed which corresponds to the loss of one bpe linker. Upon further heating another bpe was released at ~350 °C, and then decomposed to unidentified product. The PXRD pattern of dehydrated solid $\{[M(bpe)(N(CN)_2)_2]N(CN)_2\}_n$ of **1** (*i.e* **1a**) and **2** (*i.e* **2a**) exhibits no significant change compared to that of as-synthesized **1** suggesting structural rigidity of the framework (Fig. S5, ESI† and Fig. 5a–c).

Crystal-to-crystal transformations; 3D to 3D and 3D to 1D

Encouraged by the high thermal stability and structural rigidity we carried out a single-crystal-to-single-crystal transformation experiment for compound **1**. A few good quality block shaped

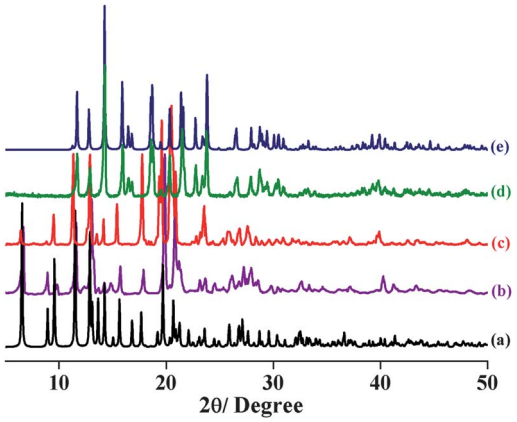

Fig. 5 PXRD patterns of **2** in different states: (a) simulated, (b) as-synthesized, (c) heated at 75 °C, (d) heated at 200 °C, (e) simulated **2b**.

single crystals of **1** were heated at 70 °C under vacuum for 12 h and we obtained a partially guest removed structure, $\{[Zn(bpe)_2(N(CN)_2)]N(CN)_2 \cdot H_2O\}_n$ (**1′**). Except for a negligible change in cell volume, other cell parameters (Table 1) remain unchanged, and single-crystal structure determination suggests that four guest water molecules were removed from hexagonal channels of the 3D porous framework. The Zn(II)–N bond length of the metal coordination sphere is in the range 2.162(5)–2.217(4) Å (Table S3, ESI†), indicating a slight increase compared to its as-synthesized solvated analogue. Here each Zn(II) centre is more close to the perfect octahedral geometry compared to the parent compound **1** which is reflected by the *cisoid* and *transoid* angles (Table S3, ESI†). The nearest neighbor Zn(II)···Zn(II) separation along dicyanamide and bpe bridges are 8.787 and 13.683 Å, respectively, and show a slight increase in distances compared to **1** suggesting some relaxation in the framework after partial removal of guest water molecules. Similar to the parent crystal structure there is a disorder in guest and bridged $N(CN)_2^-$ linkers. It is worth mentioning that complete removal of water molecules did not materialize due to instability of the single crystals. When the partially dehydrated crystals were exposed to water vapour for 1–2 days the virgin as-synthesized $\{[Zn(bpe)_2(N(CN)_2)]N(CN)_2 \cdot 5H_2O)\}_n$ (**1″**) compound was regenerated with the same composition of the parent compound **1**. X-Ray structure determination shows almost identical cell parameters (Table 1 and Table S4, ESI†) with preservation of the overall 3D framework structure as for compound **1** suggesting a reversible single-crystal-to-single-crystal structural transformation. This structural reversibility is strongly correlated to the robustness of the 3D framework.

Furthermore, the stepwise release of the coordinated bpe linkers in **1** and **2** prompted us to characterize the thermally isolated product after removal of the one bpe linker. As TGA suggests a large plateau in the range of ~200–300 °C after removal of one bpe in both cases, we have able to isolate the compound after heating **1** and **2** at ~200 °C under vacuum for 6 h. We observed a distinct color change from white to light brown (for **1**) and orange to red (for **2**) after removal of one bpe, and elemental analysis suggests the formulation of $[M(bpe)(N(CN)_2)_2]_n$ (M = Zn(II) (**1b**)/Co(II) (**2b**)) (*vide supra*). IR spectrum of the thermally isolated product of **1** shows significant changes in peak positions in particular ν(CN) which shifted to higher wavenumber indicating the coordination of both $N(CN)_2^-$ anions (Fig. S6, ESI†). The PXRD pattern of thermally isolated product (**1b** and **2b**) is completely different compared to the as-synthesized product **1** and **2**), suggesting structural transformation and reorganization after removal of the one bpe molecule (Fig. 4 and Fig. 5d and e). To get a better insight of the structures of **1b** and **2b**, the powder patterns of thermally isolated products at 200 °C were indexed by TREOR 90 program[22] and it suggests similar cell parameters to the 1D coordination chain of $[M(bpe)(N(CN)_2)_2]_n$ (M = Zn(II)/Co(II)) (cell parameters for **1b**: $a = 16.5107(4)$, $b = 9.5342(5)$, $c = 12.8793(7)$ Å, $\beta = 123.444(7)°$, $V = 1699.39(9)$ Å; **2b**: $a = 16.5034(9)$, $b = 9.5213(4)$, $c = 12.8964(6)$ Å, $\beta = 123.484(3)°$, $V = 1690.15(6)$ Å^3, see details in ESI†), which have been reported earlier.[23] We have also prepared single crystals following the same composition of **1b** and **2b** and good quality crystals were isolated after one week (see ESI†). Most interestingly X-ray single crystal diffraction suggests that the structure of **1b** or **2b** is a 1D linear coordination chain bridged by two $N(CN)_2^-$ and one bpe linkers where the bpe linker adopts *gauche* conformation to connect two Zn(II)/Co(II) centers. The torsion angle between the ethane C–C bond is about 46.93(4)° for **1b** and ~46.93(4)° for **2b** (Fig. 4 and Fig. S7 and S8, ESI†). This unprecedented structural transformation is realized by the release of one bpe linker and concurrent coordination of the non-coordinated $N(CN)_2^-$ anion and conformational change to *gauche* from *anti* of the other bpe linker for the stabilization of the resulting 1D structure.

Selective CO_2 adsorption

Encouraged by its high thermal stability and structural rigidity, dehydrated solid **2a** was subjected to gas adsorption study. After heating the compound at 75 °C under vacuum a CO_2 (kinetic diameter, 3.3 Å),[24] the adsorption isotherm was run at 195 K, and rapid onset of CO_2 adsorption was observed at very low pressure attributed to the microporosity of the compound (Fig. 6a). The final CO_2 uptake volume is 36 mL g^{-1} at P/P_0 ~1 which corresponds to 70 mg g^{-1} of CO_2 (see Fig. S9, ESI†; CO_2

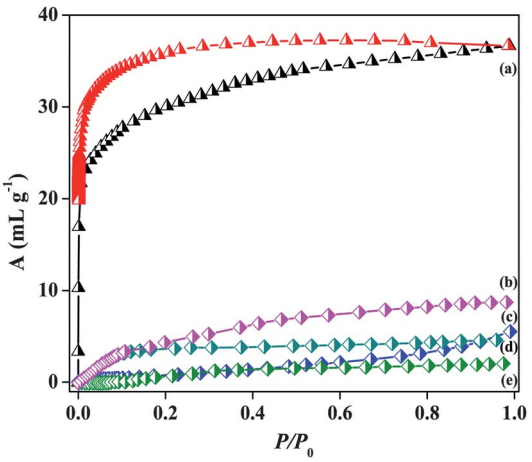

Fig. 6 Adsorption–desorption isotherm for compound **2a** at 195 K. (a) CO_2 adsorption (black) and desorption (red), adsorption profile of (b) O_2, (c) N_2, (d) Ar, (e) H_2.

adsorption isotherm of compound **1a**). The Langmuir surface area is about 180 $m^2 g^{-1}$ and the corresponding BET surface area is 137 $m^2 g^{-1}$. A distinct hysteresis in the adsorption–desorption isotherm suggests stronger interaction of CO_2 with pore surfaces which is also reflected in considerably high isosteric heat of adsorption ($\sim$ 35 kJ mol^{-1}) as calculated from the Dubinin–Radushkevich (DR) equation.[25] Stronger interaction can be attributed to the presence of nitrogen atoms of $N(CN)_2^-$ and pyridine groups of bpe on the pore walls which can interact effectively with the quadruple moment of CO_2. To our surprise, at 195 K compound **2a** shows negligible uptake of N_2 (kinetic diameter, 3.64 Å), O_2 (3.46 Å), H_2 (2.83 Å) and Ar (3.5 Å) (Fig. 6). Although the channel size is large compared to the kinetic diameter of each adsorbate, suggesting the observed selectivity is pore size independent. It is worth mentioning that N_2 and H_2 uptake was also not observed at 77 K. This is one of rare example where the diffusion of CO_2 inside the pore is solely depending upon the adsorbate–adsorbent interactions.

Excellent selectivity in gas uptake prompted us to study the vapor sorption in **2a** of different solvent molecules having different polarity and size; H_2O (kinetic diameter, 2.65 Å),[24] MeOH (4.0 Å) and EtOH (4.3 Å) (Fig. 7). The H_2O adsorption profile exhibits a two step uptake; up to relative pressure P/P_0 $\sim$0.58 it shows almost type-I profile and then steep uptake is observed up to P/P_0 $\sim$0.9 (Fig. 7c). The final uptake amount is $\sim$110 mL g^{-1} without saturation which corresponds to $\sim$2.7 molecules of H_2O per formula unit of **2a**. The MeOH profile exhibits single-step gated adsorption whereas the EtOH profile reveals gradual uptake with increasing pressure (Fig. 7b and c). Up to P/P_0 $\sim$0.42, the MeOH profile shows almost negligible uptake and the adsorption amount increases with increasing pressure and finishes with a final amount of 80 mL g^{-1} suggesting about 2.14 molecules occluded into the framework per formula unit. The 1.57 molecules of EtOH included per formula unit of **2a** correlates with that the uptake amount is in accordance to the size and polarity of the guest molecules. The desorption curve in all cases does not follow the adsorption one and shows distinct hysteresis indicating strong interaction with the pore walls. It is worth noting that such guest dependent two-step or gated adsorption behavior may be correlated to the different adsorption sites in the framework and is not related to the 'pore blocking' or 'structural breathing affect' observed in other MOF systems exhibiting stepwise or gated adsorption profile.[26]

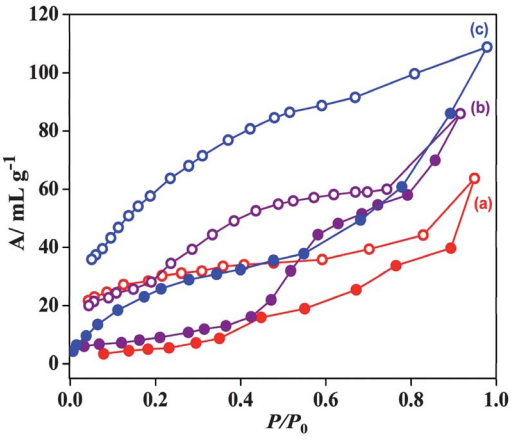

Fig. 7 Vapor adsorption–desorption isotherm for **2a**; (a) EtOH (red) at 298 K, (b) MeOH (purple) at 293 K and (c) H_2O (blue) at 298 K; P_0 is the saturated vapor pressure; 3.17 kPa (H_2O), 16.94 kPa (MeOH), 7.87 kPa (EtOH); (filled circles: adsorption, open circles: desorption).

Conclusion

In conclusion, we have synthesized two isostructural flexible porous two-fold interpenetrated 3D frameworks (**1** and **2**) with bimodal channels and upon heating both frameworks show stepwise release of guest water molecules and bpe linkers. Compound **1** shows reversible single-crystal-to-single-crystal transformation upon removal and inclusion of guest water molecules. Most significantly, for the first time, we have observed a 3D to 1D structural transformation by removal of a metal bound bridging bpe linker and concomitant bridging of non-coordinated $N(CN)_2^-$ anion and conformational change from *anti* to *gauche* of the another bpe linker. Such a structural and dimensionality change by external stimuli in a MOF would pave the way for fabrication of novel coordination frameworks having substantial importance in the field of crystal growth and engineering. The dehydrated phase of cobalt compound **2a** shows remarkable selectivity of CO_2 over a number of adsorbates (N_2, O_2, H_2 and Ar) at 195 K.

Acknowledgements

T. K. M. gratefully acknowledges the financial support from DST, Govt. of India (Fast Track Proposal). R. H. acknowledges DST, JNCASR, India.

References

1 (*a*) G. Férey, *Chem. Soc. Rev.*, 2008, **37**, 191; (*b*) S. Kitagawa, R. Kitaura and S.-I. Noro, *Angew. Chem., Int. Ed.*, 2004, **43**, 2334; (*c*) T. K. Maji and S. Kitagawa, *Pure Appl. Chem.*, 2007, **79**, 2155.

2 (*a*) H. K. Chae, M. Eddaoudi, J. Kim, S. I. Hauck, J. F. Hartwig, M. O'Keeffe and O. M. Yaghi, *J. Am. Chem. Soc.*, 2001, **123**, 11482; (*b*) M. Eddaoudi, D. B. Moler, H. L. Li, B. L. Chen, T. M. Reineke, M. O'Keeffe and O. M. Yaghi, *Acc. Chem. Res.*, 2001, **34**, 319; (*c*) L. Pan, B. Parker, X. Huang, D. H. Olson, J. Y. Lee and J. J. Li, *J. Am. Chem. Soc.*, 2006, **128**, 4180; (*d*) R. Matsuda, R. Kitaura, S. Kitagawa, Y. Kubota, R. V. Belosludov, T. C. Kobayashi, H. Sakamoto, T. Chiba, M. Takata, Y. Kawazoe and Y. Mita, *Nature*, 2005, **436**, 238; (*e*) P. Kanoo, R. Matsuda, M. Higuchi, S. Kitagawa and T. K. Maji, *Chem. Mater.*, 2009, **21**, 5861; (*f*) P. Kanoo, K. L. Gurunatha and T. K. Maji, *J. Mater. Chem.*, 2010, **20**, 1322; (*g*) S. Q. Ma, D. F. Sun, J. M. Simmons, C. D. Collier, D. Q. Yuan and H. C. Zhou, *J. Am. Chem. Soc.*, 2008, **130**, 1012; (*h*) Z. Q. Wang and S. M. Cohen, *J. Am. Chem. Soc.*, 2009, **131**, 16675; (*i*) H. J. Choi, M. Dincá and J. R. Long, *J. Am. Chem. Soc.*, 2008, **130**, 7848; (*j*) T. Ahnfeldt, N. Guillou, D. Gunzelmann, I. Margiolaki, T. Loiseau, G. Férey, J. Senker and N. Stock, *Angew. Chem., Int. Ed.*, 2009, **48**, 5163.

3 (*a*) H. K. Liu, W. Y. Sun, W. X. Tang, T. Yamamoto and N. Ueyama, *Inorg. Chem.*, 1999, **38**, 6313; (*b*) N. Guillou, P. M. Forster, Q. Gao, J. S. Chang, M. Nogues, S. E. Park, A. K. Cheetham and G. Férey, *Angew. Chem., Int. Ed.*, 2001, **40**, 2831; (*c*) S. Horike, M. Dincá, K. Tamaki and J. R. Long, *J. Am. Chem. Soc.*, 2008, **130**, 5854; (*d*) S. Hasegawa, S. Horike, R. Matsuda, S. Furukawa, K. Mochizuki, Y. Kinoshita and S. Kitagawa, *J. Am. Chem. Soc.*, 2007, **129**, 2607; (*e*) S. R. Venna and M. A. Carreon, *J. Am. Chem. Soc.*, 2010, **132**, 76; (*f*) Y. S. Li, F. Y. Liang, H. Bux, A. Feldhoff, W. S. Yang and J. Caro, *Angew. Chem., Int. Ed.*, 2010, **49**, 548; (*g*) S. Couck,

J. F. M. Denayer, G. V. Baron, T. Remy, J. Gascon and F. Kapteijn, *J. Am. Chem. Soc.*, 2009, **131**, 6326.
4 (*a*) J. Fan, W. Y. Sun, T.-A. Okamura, J. Xie, W.-X. Tang and N. Okamura, *New J. Chem.*, 2002, **26**, 199; (*b*) A. N. Parvulescu, G. Marin, K. Suwinska, V. C. Kravtsov, M. Andruh, V. Parvulescu and V. I. J. Parvulescu, *J. Mater. Chem.*, 2005, **15**, 4234; (*c*) S. Muthu, J. H. K. Yip and J. J. Vittal, *J. Chem. Soc., Dalton Trans.*, 2002, 4561; (*d*) M. H. Alkordi, Y. L. Liu, R. W. Larsen, J. F. Eubank and M. Eddaoudi, *J. Am. Chem. Soc.*, 2008, **130**, 12639; (*e*) C. Y. Sun, S. X. Liu, D. D. Liang, K. Z. Shao, Y. H. Ren and Z. M. Su, *J. Am. Chem. Soc.*, 2009, **131**, 1883.
5 (*a*) P. Horcazada, C. Serre, M. Sebban, F. Taulelle and G. Férey, *Angew. Chem., Int. Ed.*, 2006, **45**, 5974; (*b*) P. Horcazada, C. Serre, G. Maurin, N. A. Ramsahye, F. Balas, M. Vallet-Regi, M. Sebban, F. Taulelle and G. Férey, *J. Am. Chem. Soc.*, 2008, **130**, 6774; (*c*) J. Y. An, S. J. Geib and N. L. Rosi, *J. Am. Chem. Soc.*, 2009, **131**, 8376; (*d*) S. R. Miller, D. Heurtaux, T. Baati, P. Horcajada, J. M. Greneche and C. Serre, *Chem. Commun.*, 2010, **46**, 4526.
6 (*a*) H. Liu, T.-H. Tsao, Y.-T. Zhang and C.-H. Lin, *CrystEngComm*, 2009, **11**, 1462; (*b*) M.-H. Zeng, X.-L. Feng, W.-X. Zhang and X.-M. Chen, *Dalton Trans.*, 2006, 5294; (*c*) M. K. Sharma, P. Lama and P. K. Bharadwaj, *Cryst. Growth Des.*, 2011, **11**, 1411; (*d*) M. K. Sharma and P. K. Bharadwaj, *Inorg. Chem.*, 2011, **50**, 1889; (*e*) A. Aijaz, P. Lama and P. K. Bharadwaj, *Inorg. Chem.*, 2010, **49**, 5883; (*f*) H. J. Choi and M. P. Suh, *J. Am. Chem. Soc.*, 2004, **126**, 15844; (*g*) O. Ohmori, M. Kawano and M. Fujita, *J. Am. Chem. Soc.*, 2004, **126**, 16292; (*h*) M. H. Zeng, X. L. Feng and M. X. Chen, *Dalton Trans.*, 2004, 2217; (*i*) Y. X. Zhang, B. L. Chen, F. R. Fronczek and A. W. Maverick, *Inorg. Chem.*, 2008, **47**, 4433.
7 (*a*) S. Henke, R. Schmidt and J. D. Grunwaldt, *Chem.–Eur. J.*, 2010, **16**, 14296; (*b*) Z. Q. Wang and S. M. Cohen, *J. Am. Chem. Soc.*, 2009, **131**, 16675.
8 (*a*) G. Mahmoudi and A. Morsali, *Cryst. Growth Des.*, 2008, **10**, 1742; (*b*) A. Aslani and A. Morsali, *Chem. Commun.*, 2008, 3402; (*c*) A. Aslani, M. Zeller and A. Morsali, *Dalton Trans.*, 2008, 5173; (*d*) M. Khanpour and A. Morsali, *CrystEngComm*, 2009, **11**, 2585; (*e*) K. J. Wei, J. Ni, Y. S. Xie and Q. L. Liu, *Inorg. Chem. Commun.*, 2007, **10**, 279; (*f*) P. Kanoo, K. L Gurunatha and T. K. Maji, *Cryst. Growth Des.*, 2009, **9**, 4147.
9 (*a*) C. Y. Chen, P. Y. Cheng, H. H. Wu and H. M. Lee, *Inorg. Chem.*, 2007, **46**, 5691; (*b*) K. L. Gurunatha, G. Mostafa, D. Ghoshal and T. K. Maji, *Cryst. Growth Des.*, 2010, **10**, 2483; (*c*) M. H. Zeng, X. L. Feng and X. M. Chen, *Dalton Trans.*, 2004, 2217; (*d*) D. M. Shin, I. S. Lee, D. Cho and Y. K. Chung, *Inorg. Chem.*, 2003, **42**, 7722.
10 (*a*) IPCC, *IPCC Special Report on Carbon Dioxide Capture and Storage*, Cambridge University Press, Cambridge, 2005; (*b*) R. S. Haszeldine, *Science*, 2009, **325**, 1647.
11 (*a*) J. R. Li, R. J. Kuppler and H. C. Zhou, *Chem. Soc. Rev.*, 2009, **38**, 1477; (*b*) Y. Inubushi, S. Horika, T. Fukushima, G. Akiyama, R. Matsuda and S. Kitagawa, *Chem. Commun.*, 2010, **46**, 9229; (*c*) H. Wu, R. S. Reali, D. A. Smith, M. C. Trachtenberg and J. Li, *Chem.–Eur. J.*, 2010, **16**, 13951; (*d*) S. Mohapatra, K. P. S. S. Hembram, U. Waghmore and T. K. Maji, *Chem. Mater.*, 2009, **21**, 5406.
12 (*a*) T. Fukushima, S. Horike, Y. Inubushi, K. Nakagawa, Y. Kubota, M. Takata and S. Kitagawa, *Angew. Chem., Int. Ed.*, 2010, **49**, 4820; (*b*) S. R. Caskey, A. G. Wong-Foy and A. J. Matzger, *J. Am. Chem. Soc.*, 2008, **130**, 10870; (*c*) R. Vaidhyanathan, S. S. Iremonger, K. W. Dawson and G. K. H. Shimizu, *Chem. Commun.*, 2009, 5230; (*d*) R. Dey, R. Haldar, T. K. Maji and D. Ghoshal, *Cryst. Growth Des.*, 2011, **11**, 3905; (*e*) P. Kanoo, R. Haldar, S. T. Cyrac and T. K. Maji, *Chem. Commun.*, 2011, **47**, 11038.
13 T. K. Maji, R. Matsuda and S. Kitagawa, *Nat. Mater.*, 2007, **6**, 142.
14 *SMART (V 5.628), SAINT (V 6.45a), Xprep, SHELXTL*; Bruker AXS Inc. Madison, Wisconsin, USA, 2004.
15 G. M. Sheldrick, *Siemens Area Detector Absorption Correction Program*, University of Götingen, Götingen, Germany, 1994.
16 A. Altomare, G. Cascarano, C. Giacovazzo and A. Gualaradi, *J. Appl. Crystallogr.*, 1993, **26**, 343.
17 G. M. Sheldrick, *SHELXL-97, Program for Crystal Structure Solution and Refinement*, University of Götingen, Götingen, Germany, 1997.
18 A. L. Spek, *J. Appl. Crystallogr.*, 2003, **36**, 7.
19 G. M. Sheldrick, *SHELXS 97, Program for the Solution of Crystal Structure*, University of Götingen, Germany, 1997.
20 L. J. Farrugia, WinGX-A Windows Program for Crystal Structure Analysis, *J. Appl. Crystallogr.*, 1999, **32**, 837.
21 The sizes of the channels were calculated considering the van der Waals radii of the atoms.
22 P.-E. Warner, L. Eriksson and M. Westdahl, *J. Appl. Crystallogr.*, 1985, **18**, 367.
23 (*a*) N. D. Pinta, K. Urtiaga, M. G. Barandika, M. I. Arriortua, L. Lezama, G. Madariaga and R. Cartés, *Inorg. Chem.*, 2010, **49**, 10445; (*b*) J. Carranza, C. Brennan, J. Sletten, F. Lloret and M. Julve, *J. Chem. Soc., Dalton Trans.*, 2002, 3164; (*c*) S. C. Manna, E. Zangrando, J. Ribas and N. R. Chaudhuri, *Eur. J. Inorg. Chem.*, 2008, 1400.
24 C. E. Webster, R. S. Drago and M. C. Zerner, *J. Am. Chem. Soc.*, 1998, **120**, 5509.
25 M. M. Dubinin, *Chem. Rev.*, 1960, **60**, 235.
26 (*a*) P. Kanoo, R. Sambhu and T. K. Maji, *Inorg. Chem.*, 2011, **50**, 400; (*b*) J. T. Culp, M. R. Smith, E. Bittner and B. Bockroth, *J. Am. Chem. Soc.*, 2008, **130**, 12427.

